NACA

RESEARCH MEMORANDUM

ALTITUDE-WIND-TUNNEL INVESTIGATION OF A 4000-POUND-THRUST AXIAL-FLOW TURBOJET ENGINE

V - ANALYSIS OF TURBINE PERFORMANCE

By Richard P. Krebs and Reece V. Hensley

Flight Propulsion Research Laboratory
Cleveland, Ohio

NATIONAL ADVISORY COMMITTEE
FOR AERONAUTICS

WASHINGTON
August 4, 1948

NACA RM No. E8F09d RESTRICTED

NATIONAL ADVISORY COMMITTEE FOR AERONAUTICS

RESEARCH MEMORANDUM

ALTITUDE-WIND-TUNNEL INVESTIGATION OF A 4000-POUND-THRUST AXIAL-FLOW TURBOJET ENGINE

V - ANALYSIS OF TURBINE PERFORMANCE

By Richard P. Krebs and Reece V. Hensley

SUMMARY

Performance characteristics of the turbine of a 4000-pound-thrust axial-flow turbojet engine were determined in investigations of the complete engine in the NACA Cleveland altitude wind tunnel. Characteristics are presented as functions of the total-pressure ratio across the turbine and of turbine speed and gas flow corrected to sea-level conditions.

Three turbine nozzles of different areas were used to determine the area that gave optimum performance. Inasmuch as tail-pipe nozzles of different diameters were investigated in combination with the standard turbine nozzle, the effect of varying discharge conditions on turbine operation could be observed.

The investigations covered a range of pressure altitudes from 5000 to 40,000 feet. The engine was investigated over the entire operable range of speeds at each altitude. At a pressure altitude of 30,000 feet, the effect on turbine operation of varying the ram pressure ratio over a range from 1.10 to 1.77 was evaluated.

An altitude effect was apparent when turbine pressure ratio was plotted against corrected turbine speed but it was so slight as to be negligible insofar as the turbine efficiencies were concerned. A maximum turbine efficiency of slightly more than 82 percent was obtained with the configuration using the standard turbine nozzle and the low-flow compressor. This efficiency, which is somewhat lower than the actual turbine efficiency, is uncorrected for accessories drive power, bearing friction, tail-pipe pressure drop, compressor thermal radiation, and introduction of turbine-disk cooling air into the gas stream. Changes in the ram pressure ratio had a negligible effect on the turbine efficiency.

INTRODUCTION

An investigation of the altitude performance and the operational characteristics of the 4000-pound-thrust axial-flow turbojet engine and its component parts has been conducted in the NACA Cleveland altitude wind tunnel. Summaries of the over-all performance and operational characteristics of the engine are given in references 1 to 3 and the compressor performance is given in reference 4.

A specific objective of the research program was to study the performance of the turbine. During the runs considered herein several different turbine-nozzle and tail-pipe-nozzle configurations were used. The engine operated over a range of ram pressure ratios from 1.01 to 1.77 and pressure altitudes from 5000 to 40,000 feet. Although refrigerated air was used, the cooling capacity of the system was insufficient to maintain NACA standard temperatures for the lower ram pressure ratios at the higher altitudes.

The high-flow compressor unit reported does not represent any engine contemplated for production by the engine manufacturer, but does represent the initial attempt of the engine manufacturer to obtain increased performance by modifying the standard 4000-pound-thrust axial-flow unit with the quickest and simplest methods available at the time of the wind-tunnel research program.

An analysis of the turbine performance and the effect of changes in turbine-nozzle area and tail-pipe-nozzle area are given. Data are presented for five configurations involving two different compressors, three sizes of turbine nozzle, and three tail-pipe nozzles of different areas.

SYMBOLS

The following symbols are used in this report:

A	cross-sectional area, square feet
a	velocity of sound in gas, feet per second
c_p	specific heat at constant pressure, Btu per pound $^{\circ}R$
c_v	specific heat at constant volume, Btu per pound $^{\circ}R$
g	ratio of absolute to gravitational units of mass, (32.17)
J	mechanical equivalent of heat, foot-pounds per Btu, (778)

k constant

M Mach number

N engine speed, rpm

P total pressure, pounds per square foot

p static pressure, pounds per square foot

R gas constant, foot-pounds per pound $^{\circ}R$, (53.3)

T total temperature, $^{\circ}R$

T_i indicated temperature, $^{\circ}R$

t static temperature, $^{\circ}R$

u turbine rotor tip speed, feet per second

V velocity of gas flow, feet per second

v turbine-nozzle jet velocity, feet per second

W_g gas flow, pounds per second

α thermocouple impact recovery factor

γ ratio of specific heats, c_p/c_v

δ_5 pressure correction factor, $P_5/2116$ (turbine-inlet total pressure divided by NACA standard sea-level pressure)

η_t turbine efficiency, percent

θ_5 temperature correction factor, $\gamma_5 T_5/1.40 \times 519$ (product of γ and total temperature at turbine inlet divided by product of γ and total temperature for air at NACA standard sea-level conditions)

ρ static density, pounds per cubic foot

Subscripts:

c compressor

n turbine-nozzle throat

t turbine

5 station at turbine inlet

6 station at turbine outlet

7 station at junction of tail pipe and tail-pipe nozzle

8 station at tail-pipe-nozzle outlet

DESCRIPTION OF TURBINE

The J35 turbojet engine is equipped with a single-stage impulse turbine (fig. 1), which delivers about 7000 horsepower at rated engine conditions (7600 rpm at NACA standard sea-level conditions).

The turbine is equipped with a diaphragm-type nozzle. Three nozzles, differing only in throat area, were used in the investigation and are identified as follows: small turbine nozzle, 1.101.9 101.9 square inches; standard turbine nozzle, 106.8 square inches; and large turbine nozzle, 121.0 square inches. The turbine-nozzle vanes, which are 3.15 inches long, are fixed at both ends and leave no space for gas leakage around the nozzle box. The inner diameter of the flow annulus is 26.96 inches. The axial distance between the nozzle outlet and the turbine rotor is 0.449 inch.

The turbine-disk diameter is 27 inches. The disk thickness decreases from 3.94 inches at the drive shaft to 0.565 inch at a radius of 11.5 inches and then abruptly increases to 1.562 inches at the periphery. The rotor blades are solid and are welded to the periphery of the rotor disk. The rotor blades are 3.5 inches long at the trailing edge and decrease in length toward the leading edge. A shroud ring at the blade tips stiffens the blades and helps to prevent leakage around the rotor. The change in rotor-blade length from trailing edge to leading edge makes the shroud ring conform to the shape of the surface of a very thin frustum of a large-diameter cone, the sides of which form an angle with the drive shaft of 7.5°. The over-all diameter of the rotor including the shroud ring is 34.126 inches. The radial clearance between the shroud ring and the casing is about 0.2 inch and the axial clearance between the leading edge of the shroud ring and the side of the turbine housing is 0.095 inch.

Air for cooling the disk is piped from the eighth compressor stage to both sides of the turbine wheel and impinges on the disk

near the drive shaft. The air then travels radially outward along the turbine disk and enters the engine flow passage at the disk periphery.

INSTRUMENTATION

Instrumentation of the axial-flow-type turbojet engine investigated is discussed and illustrated in reference 1. Instrumentation was installed at the stations shown in figure 2.

The data obtained for the stations with which this report is concerned consisted of:

Total pressure at station 5 obtained by two diametrically opposite total-pressure tubes located on the leading edge of the nozzle vanes at the average radius of the turbine-nozzle annulus.

Static pressure and indicated temperature at station 6 obtained from two static wall orifices and eight uniformly spaced thermocouples located at the turbine exit.

Total pressure at station 7 measured by four equally spaced total-pressure tubes located approximately $3\frac{1}{2}$ inches from the outer shell.

Complete instrumentation of the tail-pipe-nozzle rake with sufficient total-pressure, static-pressure, and indicated-temperature measurements to give a complete survey at station 8.

Turbine-outlet thermocouples were installed at station 6 to indicate which burners were ignited. Because these thermocouples were subjected to radiation from the hot gases in the burners, the temperature readings were not suitable for turbine-performance calculations.

PROCEDURE

Investigations were conducted over the operable range of engine speeds of each configuration shown in the following table:

Configuration (a)	Compressor	Turbine-nozzle area (sq in.)	Tail-pipe-nozzle diameter (in.)	Pressure altitude (ft)	Ram pressure ratio
1	Low flow	Small, 101.9 to 97.7	$16\frac{1}{4}$	5,000 to 40,000	1.01
2	Low flow	Standard, 106.8 to 108.0	$16\frac{1}{4}$	10,000 to 30,000	1.21
3,4	Low flow	Standard, 106.8 to 108.0	$16\frac{3}{4}$	10,000 to 40,000 30,000	1.21 1.10 to 1.77
6	High flow	Standard, 106.8 to 108.0	18	20,000 to 40,000	1.39
12	High flow	Large, 121.0 to 119.8	$19\frac{1}{2}$	20,000 to 40,000	1.42

[a]Configuration numbers correspond to those given in reference 2.

During the runs the turbine nozzles were warped by heat and pressure. The values given in the turbine-nozzle-area column are the areas of the turbine nozzle at the minimum section as measured at the beginning and the end of the runs.

METHODS OF CALCULATION

Efficiency

The following equation was used for the calculation of turbine efficiency:

$$\eta_t = \frac{\Delta T_t}{T_5\left[1 - \left(\frac{P_6}{P_5}\right)^{\frac{\gamma-1}{\gamma}}\right]} \qquad (1)$$

This efficiency is based on the total-pressure drop across the turbine. No instrumentation that was considered reliable for measuring all of these quantities directly was available. Total-pressure measurements were available at stations 5 and 7. Sufficient data were available at station 8 to compute the total temperature T_8.

The enthalpy rise across the compressor was assumed equal to the enthalpy drop across the turbine, and the total temperature drop across the turbine was obtained from the relation

$$\Delta T_t = \Delta T_c \frac{c_{p,c}}{c_{p,t}} \tag{2}$$

where the mass of gas flow was assumed equal to the mass of air flow. This assumption is justified because air in a quantity approximately equal to the fuel flow was bled from the fourth stage of the compressor to cool the bearings. This air was then discharged from the engine. The turbine-disk cooling air does not enter these considerations because it becomes a part of the general engine gas flow.

The total temperature at the turbine outlet T_6 was assumed equal to T_8 and the total pressure at the turbine outlet P_6 was assumed equal to P_7. The swirl at the turbine outlet encumbered the measurement of total pressure at station 6. More accurate measurements of total pressure could be made at station 7 where the flow was more uniform and the swirl less; however, there was a total-pressure loss caused by the friction of the gas flow in the tail pipe. This loss was charged to the turbine, thereby lowering the computed turbine efficiency.

The total temperature at the turbine inlet T_5 was computed by

$$T_5 = \Delta T_t + T_6 \tag{3}$$

The value of γ was determined from a curve using the values of the fuel-air ratio, the average turbine total temperature, and an assumed combustion efficiency of 98 percent.

In addition to the work put into the compressor, the work output of the turbine should include compressor thermal-radiation losses and the work required to overcome bearing friction and to drive the accessories. In the computation of total-temperature drop across the turbine, however, only the work put into the compressor was considered. Although the resultant efficiency value is lower than the actual adiabatic efficiency of the turbine, it is considered sufficiently accurate to justify comparisons among the efficiencies for the different configurations investigated.

The use of $P_6 = P_7$ and the neglect of any work other than that put into the compressor tended to lower the computed turbine efficiency; whereas the introduction of cooling air through the turbine wheel tended to raise the computed turbine efficiency by lowering the calculated value of T_5.

Gas Flow

The gas flow through the turbine was calculated from pressures and temperatures measured at the tail-pipe-nozzle rake from

$$W_g = \frac{p_8 A_8}{R} \sqrt{\frac{2Jgc_p}{t_8} \left[\left(\frac{P_8}{p_8} \right)^{\frac{\gamma_8 - 1}{\gamma_8}} - 1 \right]} \tag{4}$$

Temperatures

Static temperatures were calculated from indicated temperatures by

$$t = \frac{T_i}{1 + \alpha \left[\left(\frac{P}{p} \right)^{\frac{\gamma - 1}{\gamma}} - 1 \right]} \tag{5}$$

From calibration tests of thermocouples of the type used, α was found to be equal to 0.85.

Total temperature was computed by

$$T = t + \frac{T_i - t}{0.85} \tag{6}$$

RESULTS AND DISCUSSION

The effect on the performance and the efficiency of the turbine of changes in altitude, tail-pipe-nozzle area, and ram pressure ratio is presented. Because changes in turbine-nozzle area alter the geometry of the turbine, each configuration involving a change in turbine nozzle will be separately treated.

No complete performance curves for the turbine are presented inasmuch as the data obtained cover only the range of conditions encountered with the turbine operating in the turbojet engine.

Method of Presentation

The usual method of presentation of turbine data, using the ratio of turbine tip speed to turbine-nozzle-jet velocity u/v, was considered unsiutable for the present data. Calculations of u/v were made but the range of the variable was so small that this ratio was considered an undesirable coordinate. Greater emphasis has therefore been placed on the concept of a "turbine operating line," plotted as pressure ratio P_5/P_6 against corrected gas flow $\frac{W_g \sqrt{\theta_5}}{\delta_5 \gamma_5/1.4}$. Each configuration gives sufficient data to establish an operating line. Data concerning the turbine can be obtained only at points that fall along an operating line.

The expression for corrected gas flow is developed from the following expression for Mach number:

$$M = \frac{V}{a} = \frac{W_g}{\rho A a} = \frac{W_g R t}{pA \sqrt{\gamma g R t}} \tag{7}$$

When the equation is changed from static to total values of pressure and temperature

$$M = \frac{W_g}{A} \sqrt{\frac{R}{\gamma g}} \frac{\sqrt{T}}{P} \left(1 + \frac{\gamma - 1}{2} M^2\right)^{\frac{\gamma+1}{2(\gamma-1)}} \tag{8a}$$

or

$$\frac{\sqrt{g}\, MA}{\sqrt{R} \left(1 + \frac{\gamma - 1}{2} M^2\right)^{\frac{\gamma+1}{2(\gamma-1)}}} = \frac{W_g \sqrt{\gamma T}}{\gamma P} \tag{8b}$$

or, when corrected to standard sea-level conditions,

$$\frac{kAM}{\left(1 + \frac{\gamma - 1}{2} M^2\right)^{\frac{\gamma+1}{2(\gamma-1)}}} = \frac{W_g \sqrt{\theta}}{\delta \frac{\gamma}{1.4}} \qquad (8c)$$

The last term of equation (8c) was chosen as the expression for corrected gas flow because at a Mach number of 1 it maintains very nearly a constant value with varying temperature and pressure. For the range of γ_5 occurring in the data presented (1.385 to 1.315), $\frac{1}{\left(\frac{\gamma_5 + 1}{2}\right)^{\frac{\gamma_5+1}{2(\gamma_5-1)}}}$ increases 0.75 percent.

Effects of Altitude

The effect of altitude on turbine pressure ratio is shown in figure 3, where turbine pressure ratio is plotted against corrected turbine speed for the standard turbine nozzle and the $16\frac{1}{4}$-, $16\frac{3}{4}$-, and 18-inch-diameter tail-pipe nozzles. Figures 3(a) and 3(b) show an increase in pressure ratio with altitude at a given corrected turbine speed. The separation of the curves in each group is assumed to be an indication of the Reynolds number effect. In the case of the 18-inch tail-pipe nozzle (fig. 3(c)), the data cover a very narrow range of corrected speeds where the pressure-ratio curve is very steep and no altitude effect is apparent. No altitude effect is shown by the operating lines in figure 4, where pressure ratio is plotted against corrected gas flow.

Configurations with two turbine nozzles other than the standard nozzle were investigated: the small turbine nozzle with the low-flow compressor and a $16\frac{1}{4}$-inch tail-pipe nozzle; and the large turbine nozzle with the high-flow compressor and a $19\frac{1}{2}$-inch tail-pipe nozzle. The operating characteristics with the small turbine nozzle are shown in figure 5, and those with the large turbine nozzle are shown in figure 6. Both sets of data exhibit the same general characteristics as those for the other configurations.

Effects of Tail-Pipe-Nozzle Area

When the turbine operates at conditions such that the Mach number is 1 at the turbine-nozzle throat, equation (8c) becomes

$$\frac{W_g\sqrt{\theta_5}}{\delta_5 \frac{\gamma_5}{1.4}} = \frac{k A_n}{\left(\frac{\gamma_5 + 1}{2}\right)^{\frac{\gamma_5+1}{2(\gamma_5-1)}}} \qquad (9)$$

Sonic velocity at the throat occurs when the pressure ratio across the nozzle is greater than critical (1.85 to 1.89 depending on the value of γ_5). If it is assumed that there is no static-pressure drop through the turbine, the foregoing condition will be met when the value of P_5/p_6 exceeds the critical or when P_5/P_6 exceeds a value slightly less than this value. The corrected gas flow should be approximately constant $\left(\text{varying inversely as} \left(\frac{\gamma_5 + 1}{2}\right)^{\frac{\gamma_5+1}{2(\gamma_5-1)}}\right)$ when the pressure ratio across the turbine exceeds the critical value. The corrected gas flow should be independent of downstream conditions, except insofar as varying the back pressure on the turbine changes γ_5 through changes in the turbine-inlet temperature.

On the operating lines in figure 4, the corrected gas flow for the $16\frac{1}{4}$- and $16\frac{3}{4}$-inch tail-pipe nozzles increases about 1 percent when the turbine pressure ratios increase from 1.8 to the maximum values obtained. This increase closely checks the expected increase previously discussed.

The three operating lines for the turbine with the standard turbine nozzle and three different tail-pipe nozzles are plotted in figure 7. The operating lines for the $16\frac{1}{4}$- and $16\frac{3}{4}$-inch tail-pipe nozzles should coincide for values of P_5/P_6 greater than critical because the values of γ_5 are practically the same for both configurations. The data presented, however, show no such coincidence. Owing to lack of precision in the data, no further conclusions on the effect of tail-pipe-nozzle area on turbine operation can be made.

The operating line with the high-flow compressor and 18-inch tail-pipe nozzle is shifted to the left of the operating line with the $16\frac{1}{4}$-inch tail-pipe nozzle. Lower turbine-inlet temperatures were found with the high-flow compressor than with the low-flow compressor. The higher values of γ_5 at these lower temperatures resulted in a lower corrected gas flow.

Some shift in the operating lines for the three configurations might be attributable to changes in the turbine-nozzle area. Changes in the nozzle area of 1.1 percent from the beginning to the end of the run were caused by warping and erosion of the nozzle. Possibly greater changes in the area occurred at some time during the runs. Pitting and warping may also have contributed to a change in the flow pattern of the gas through the nozzle.

602

Effects of Ram Pressure Ratio

Variable ram tests with ram pressure ratios from 1.10 to 1.77 were made with the standard turbine nozzle and the $16\frac{3}{4}$-inch tail-pipe nozzle at a pressure altitude of 30,000 feet. The results of these tests are shown in figure 8, where turbine pressure ratio is plotted against corrected turbine speed and corrected gas flow.

The low engine-speed points for ram pressure ratios of 1.66 and 1.77 corresponded to the highest corrected turbine speed points shown (4230 rpm). As the engine speed increased, the corrected turbine speed decreased to a value slightly less than 4000 rpm; with a further increase in engine speed, the corrected turbine speed increased to approximately 4100 rpm. If the engine were operable at lower engine speeds under these conditions of altitude and ram, the experimental points would lie between the low engine-speed points shown and the points corresponding to windmilling operation of the engine. At a pressure altitude of 30,000 feet, the engine windmilled at the following conditions:

Ram pressure ratio	Corrected turbine speed, $N/\sqrt{\theta_5}$	Approximate turbine pressure ratio P_5/P_6
1.10	Not obtained	Not obtained
1.21	2650	1.10
1.66	3250	1.32
1.77	3500	1.38

In figure 8 the broken portions of the curves are extended to the windmilling regions.

Turbine Efficiency

Turbine efficiencies are plotted against turbine pressure ratio in figure 9(a). Inasmuch as no consistent altitude effect was indicated, a single curve was drawn for each configuration.

The peak turbine efficiency encountered in these runs was obtained with the standard turbine nozzle at a turbine pressure ratio approximately equal to critical. The turbine operated with a maximum efficiency of approximately 80.5 percent with the $16\frac{1}{4}$-inch tail-pipe nozzle and slightly more than 82 percent with the $16\frac{3}{4}$-inch nozzle. The entire operating range of the turbine with the 18-inch nozzle and the high-flow compressor was at pressure ratios that exceeded the critical. Above the critical pressure ratio, the occurrence of supersonic flow velocities in the nozzle discharge may lead to losses in turbine efficiency.

Efficiency contours are plotted on the three operating lines for the standard turbine nozzle in figure 7. From these contours it appears that the maximum turbine efficiency would be slightly greater than 82 percent. All the operating curves fall to the left of the region of maximum efficiency, although the maximum efficiency obtained with the $16\frac{3}{4}$-inch tail-pipe nozzle is probably near the maximum efficiency of the turbine. When the turbine with the standard turbine nozzle and the low-flow compressor operated at pressure ratios greater than 1.35, corresponding to engine speeds greater than one-half rated speed, the efficiencies obtained were within 4 percent of the maximum value found in this investigation.

Efficiencies are plotted as a function of corrected turbine speed in figure 9(b). The peak turbine efficiency with the standard turbine nozzle is reached at a corrected speed of about 3400 rpm. Because the turbine-inlet temperature increases almost linearly with engine speed at higher values, the reduction of corrected turbine speed from a maximum of 4050 to 3400 rpm corresponds to a reduction of engine speed from a maximum of 7600 to 4900 rpm; in other words, the turbine operates at maximum efficiency in the engine at approximately 0.65 rated engine speed with the standard turbine nozzle. The displacement of the efficiency curve (fig. 9(b)) for the 18-inch

tail-pipe nozzle from those for the $16\frac{1}{4}$- and $16\frac{3}{4}$-inch tail-pipe nozzles is caused by the use of the high-flow compressor. A change in compressor so affects the turbine inlet temperature, the temperature drop across the turbine, and the engine speed that a comparison of turbine efficiencies with reference to corrected speed for the two compressors is not strictly justified.

When the engine configuration was changed by the introduction of the small or large turbine nozzles, lower turbine efficiencies were generally obtained than with the standard turbine nozzle, especially in the more desirable portions of the operating range. The maximum efficiency obtained with the small turbine nozzle was about 80.5 percent. This value occurred at approximately 0.5 rated engine speed; whereas the maximum efficiency with the standard turbine nozzle occurred at about 0.65 rated engine speed. The entire range of operation with the large turbine nozzle was at pressure ratios too high to obtain a peak efficiency.

The turbine operation for all the configurations discussed is summarized in the following table:

Configuration	Maximum efficiency obtained (percent)	Efficiency at rated speed (percent)
1	80.5	(a)
2	80.5	(a)
3,4	82	79
6	78	74.5
12	77	73.5

[a]Rated speed not reached.

The turbine efficiencies for the variable-ram-pressure data obtained at a pressure altitude of 30,000 feet are plotted against the turbine pressure ratio in figure 10. The faired curve is taken from the efficiency curve for this configuration in figure 9(a). The data indicate no definite changes in turbine efficiency at various ram pressure ratios.

SUMMARY OF RESULTS

When investigated at conditions required by the over-all performance characteristics of the 4000-pound-thrust axial-flow turbojet

engine, the turbine was found to have the following operating characteristics:

1. An altitude effect was indicated by an increase in pressure ratio across the turbine with increase in altitude at constant corrected turbine speed. No altitude effect was apparent from the turbine operating line or from the efficiencies because of the scatter of the data.

2. The configuration giving maximum turbine efficiency used the standard turbine nozzle and the low-flow compressor. This maximum efficiency of slightly more than 82 percent was obtained at turbine pressure ratios approximating the critical value and an engine speed approximating 0.65 rated speed. This value, which is somewhat lower than the actual turbine efficiency, is based on a computed efficiency in which corrections for accessories drive power, bearing friction, tail-pipe pressure drop, compressor thermal radiation, and introduction of turbine-disk cooling air into the gas stream have been neglected.

3. At all speeds greater than one-half rated engine speed, the turbine with the standard nozzle and the low-flow compressor operated within 4 percent of the maximum value obtained in this investigation.

4. Changes in the ram pressure ratio had a negligible effect on the turbine efficiency.

Flight Propulsion Research Laboratory,
National Advisory Committee for Aeronautics,
Cleveland, Ohio.

REFERENCES

1. Fleming, William A.: Altitude-Wind-Tunnel Investigation of a 4000-Pound-Thrust Axial-Flow Turbojet Engine. I - Performance and Windmilling Drag Characteristics. NACA RM No. E8F09, 1948.

2. Fleming, William A.: Altitude-Wind-Tunnel Investigation of a 4000-Pound-Thrust Axial-Flow Turbojet Engine. II - Operational Characteristics. NACA RM No. E8F09a, 1948.

3. Fleming, William A., and Golladay, Richard L.: Altitude-Wind-Tunnel Investigation of a 4000-Pound-Thrust Axial-Flow Turbojet Engine. III - Performance Characteristics with the High-Flow Compressor. NACA RM No. E8F09b, 1948.

4. Dietz, R. O., and Suozzi, Frank L.: Altitude-Wind-Tunnel Investigation of a 4000-Pound-Thrust Axial-Flow Turbojet Engine. IV - Analysis of Compressor Performance. NACA RM No. E8F09c, 1948.

602

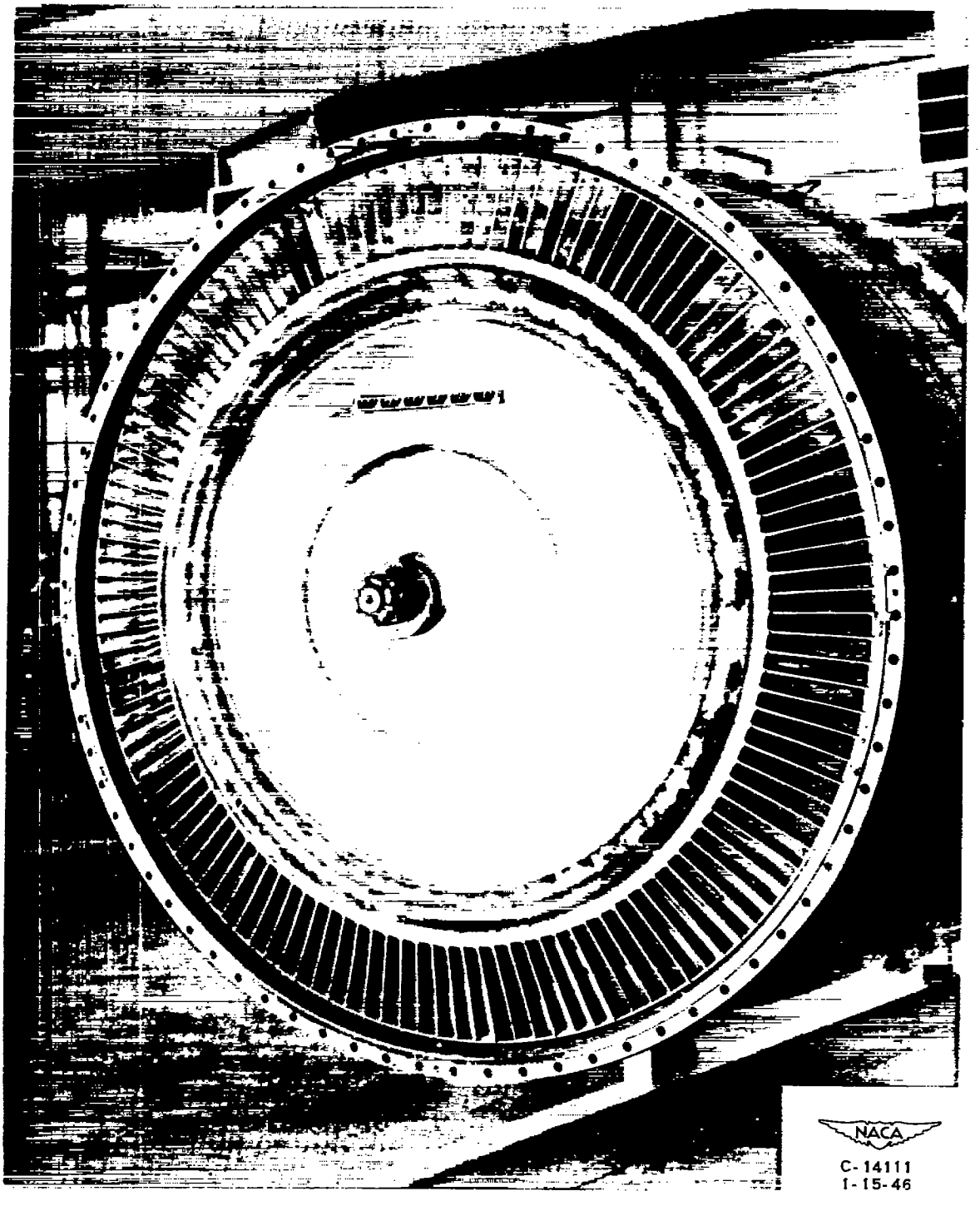

Figure 1. – Turbine installed in 4000-pound-thrust axial-flow turbojet engine with tail pipe removed.

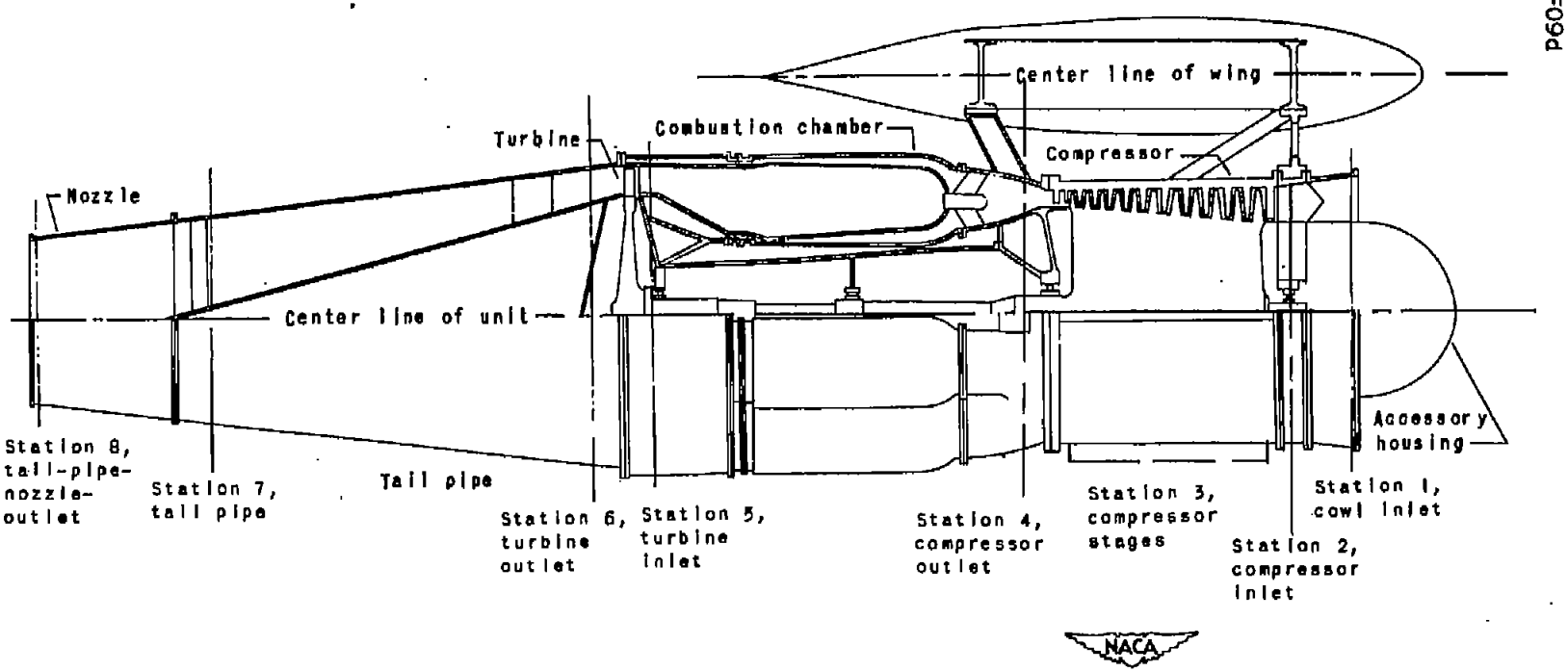

Figure 2. – Side view of 4000-pound-thrust axial-flow turbojet installation showing measuring stations.

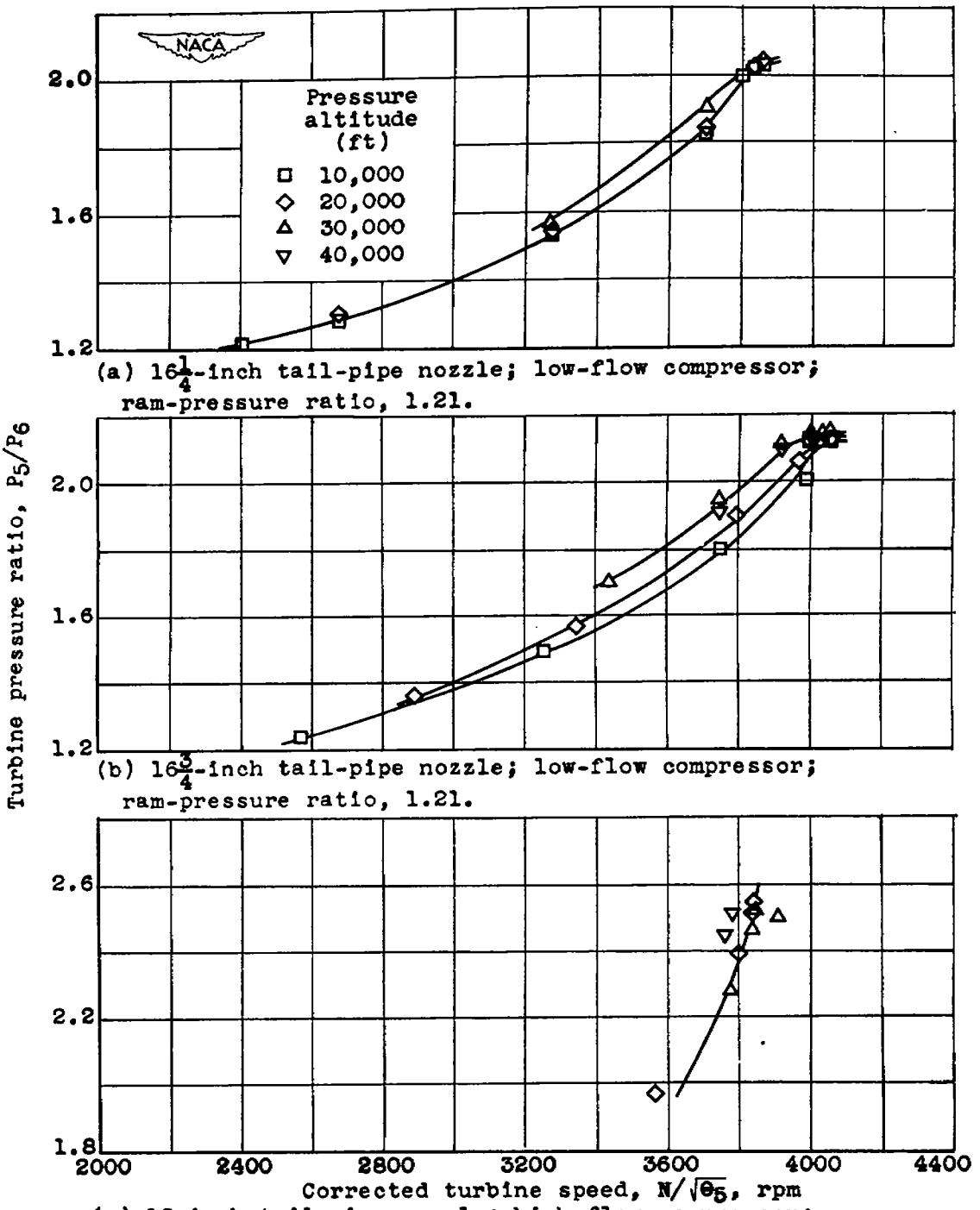

(a) $16\frac{1}{4}$-inch tail-pipe nozzle; low-flow compressor; ram-pressure ratio, 1.21.

(b) $16\frac{3}{4}$-inch tail-pipe nozzle; low-flow compressor; ram-pressure ratio, 1.21.

(c) 18-inch tail-pipe nozzle; high-flow compressor; ram-pressure ratio, 1.39.

Figure 3.- Effect of altitude on relation between turbine pressure ratio and corrected turbine speed for turbine with standard turbine nozzle. Turbine speed corrected to NACA standard atmospheric conditions at sea level.

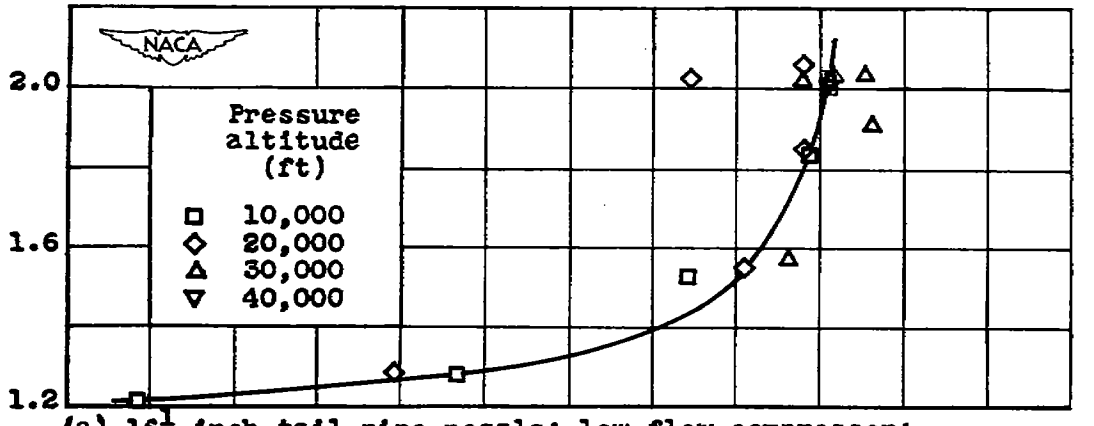

(a) $16\frac{1}{4}$-inch tail-pipe nozzle; low-flow compressor; ram-pressure ratio, 1.21.

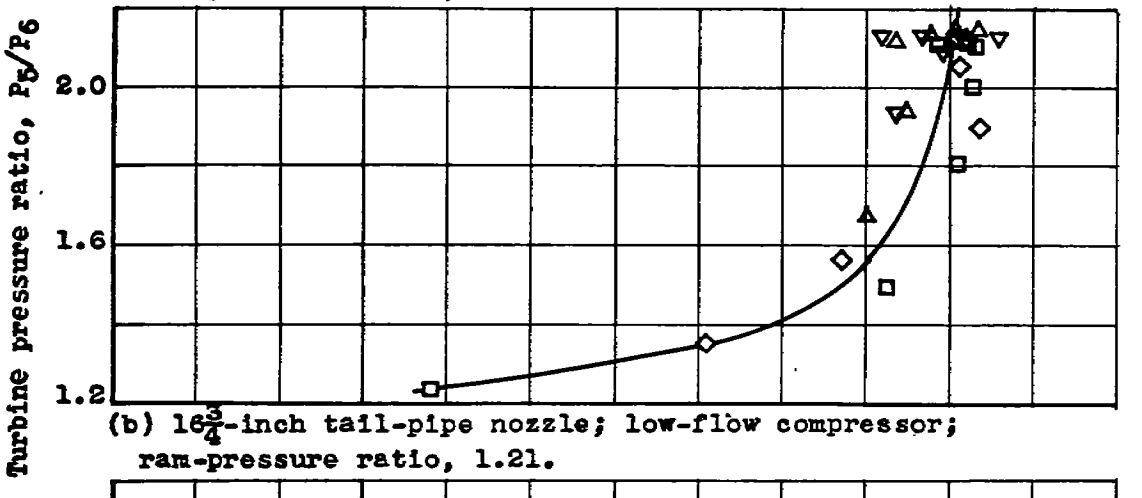

(b) $16\frac{3}{4}$-inch tail-pipe nozzle; low-flow compressor; ram-pressure ratio, 1.21.

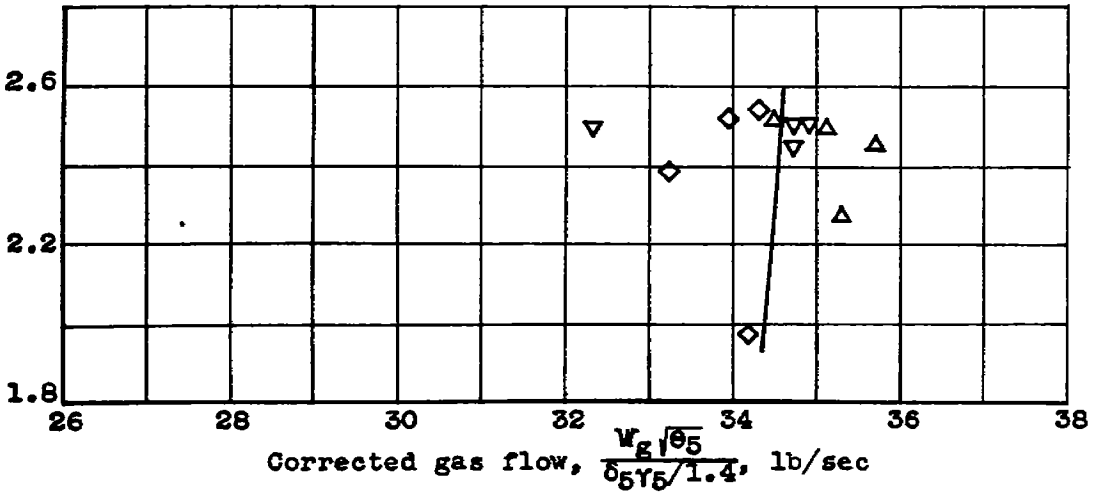

(c) 18-inch tail-pipe nozzle; high-flow compressor; ram-pressure ratio, 1.39.

Figure 4.- Operating lines for turbine with standard turbine nozzle. Gas flow corrected to NACA standard atmospheric conditions at sea level.

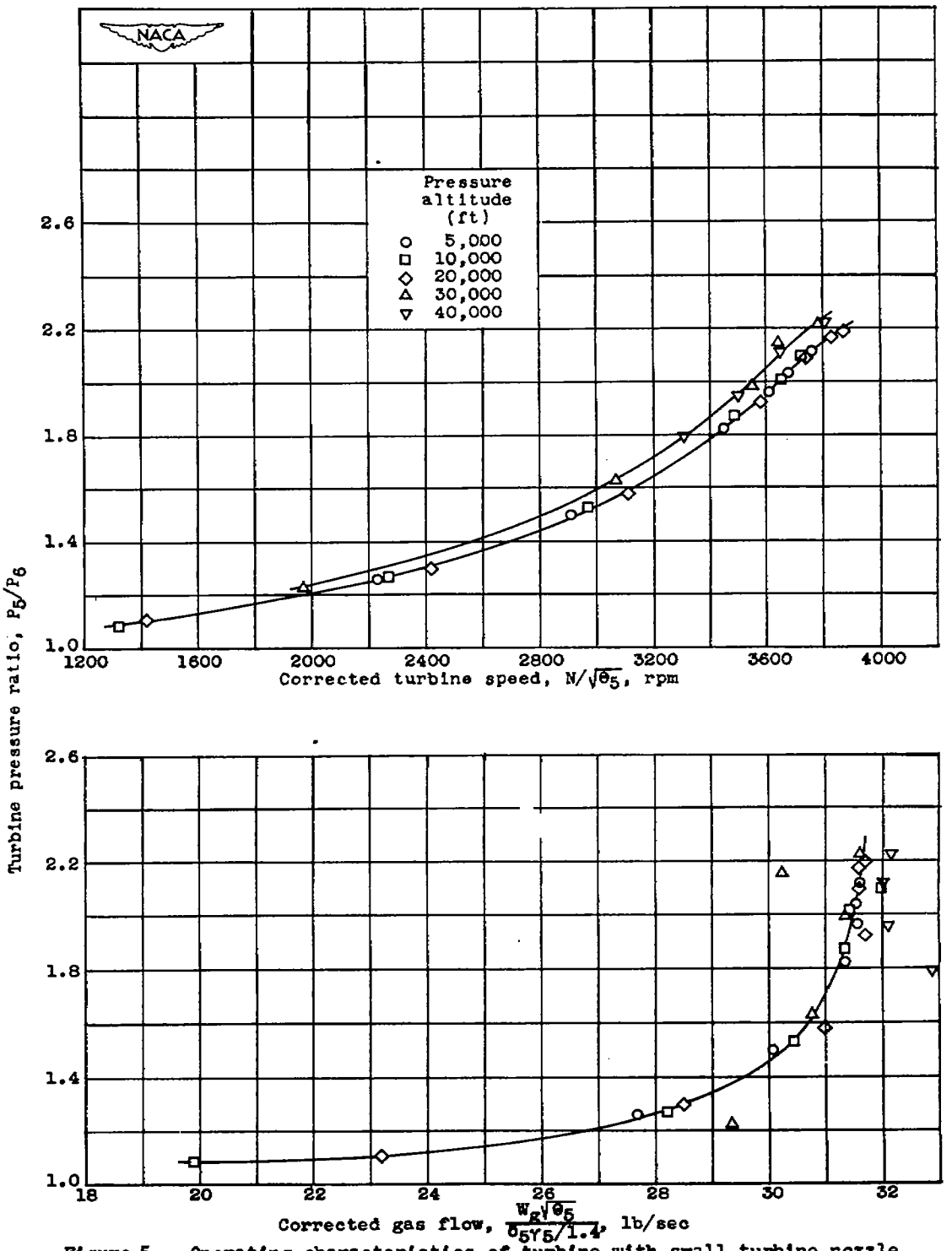

Figure 5.- Operating characteristics of turbine with small turbine nozzle, low-flow compressor, and 16¼-inch tail-pipe nozzle at a ram-pressure ratio of 1.01. Turbine speed and gas flow corrected to NACA standard atmospheric conditions at sea level.

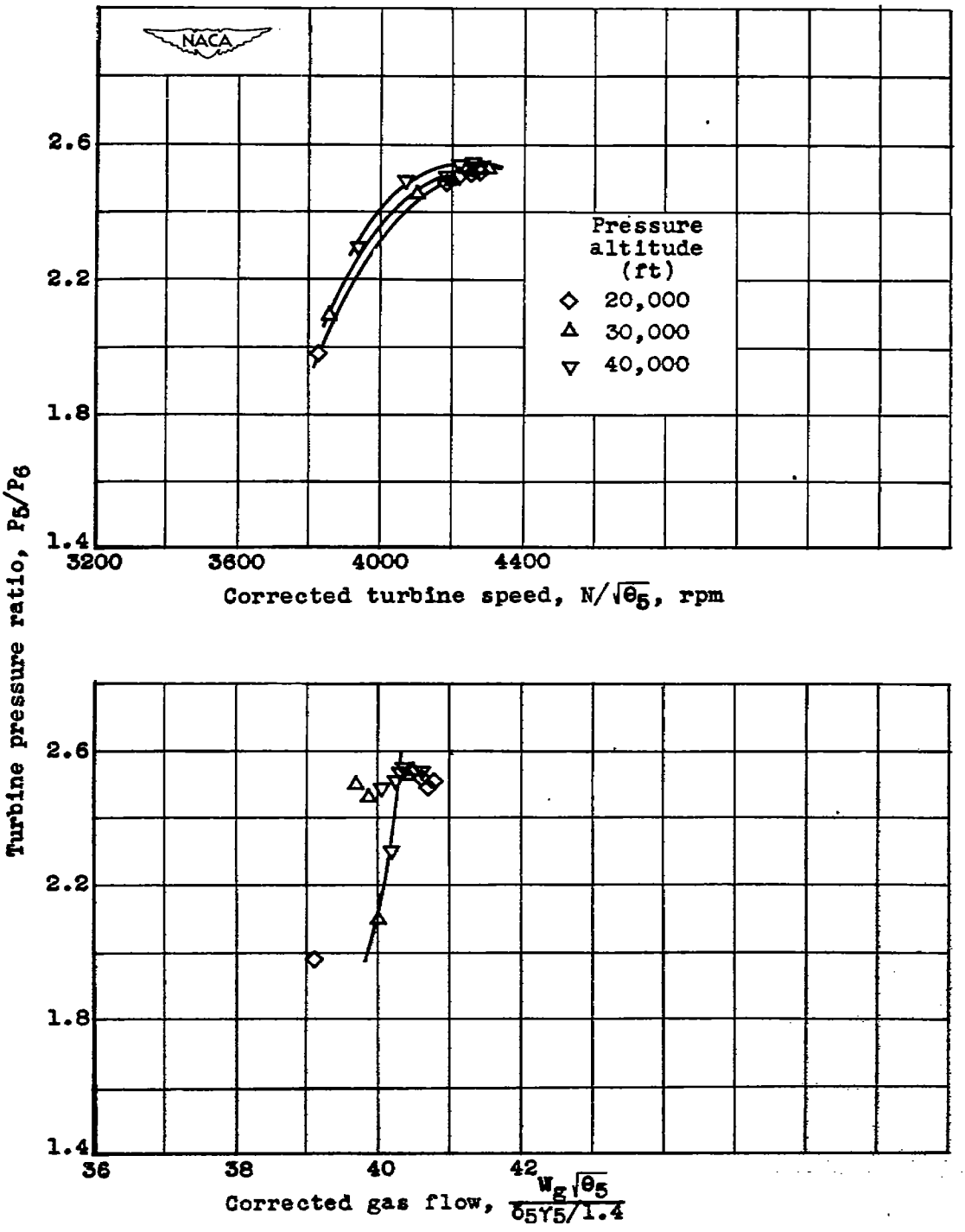

Figure 6.- Operating characteristics of turbine with large turbine nozzle, high-flow compressor, and 19½-inch tailpipe nozzle at ram-pressure ratio of 1.42. Turbine speed and gas flow corrected to NACA standard atmospheric conditions at sea level.

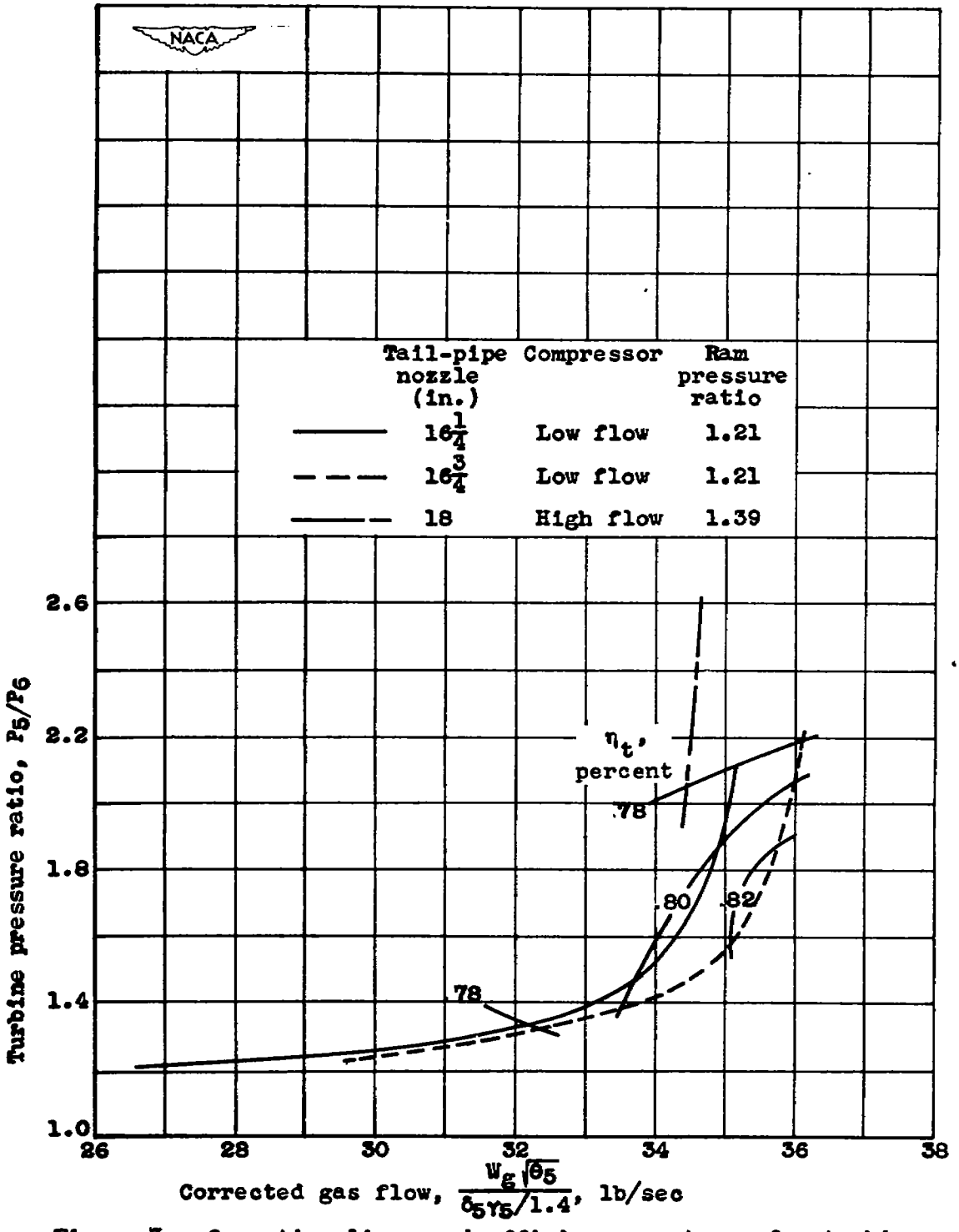

Figure 7.- Operating lines and efficiency contours for turbine with standard turbine nozzle. Gas flow corrected to NACA standard atmospheric conditions at sea level.

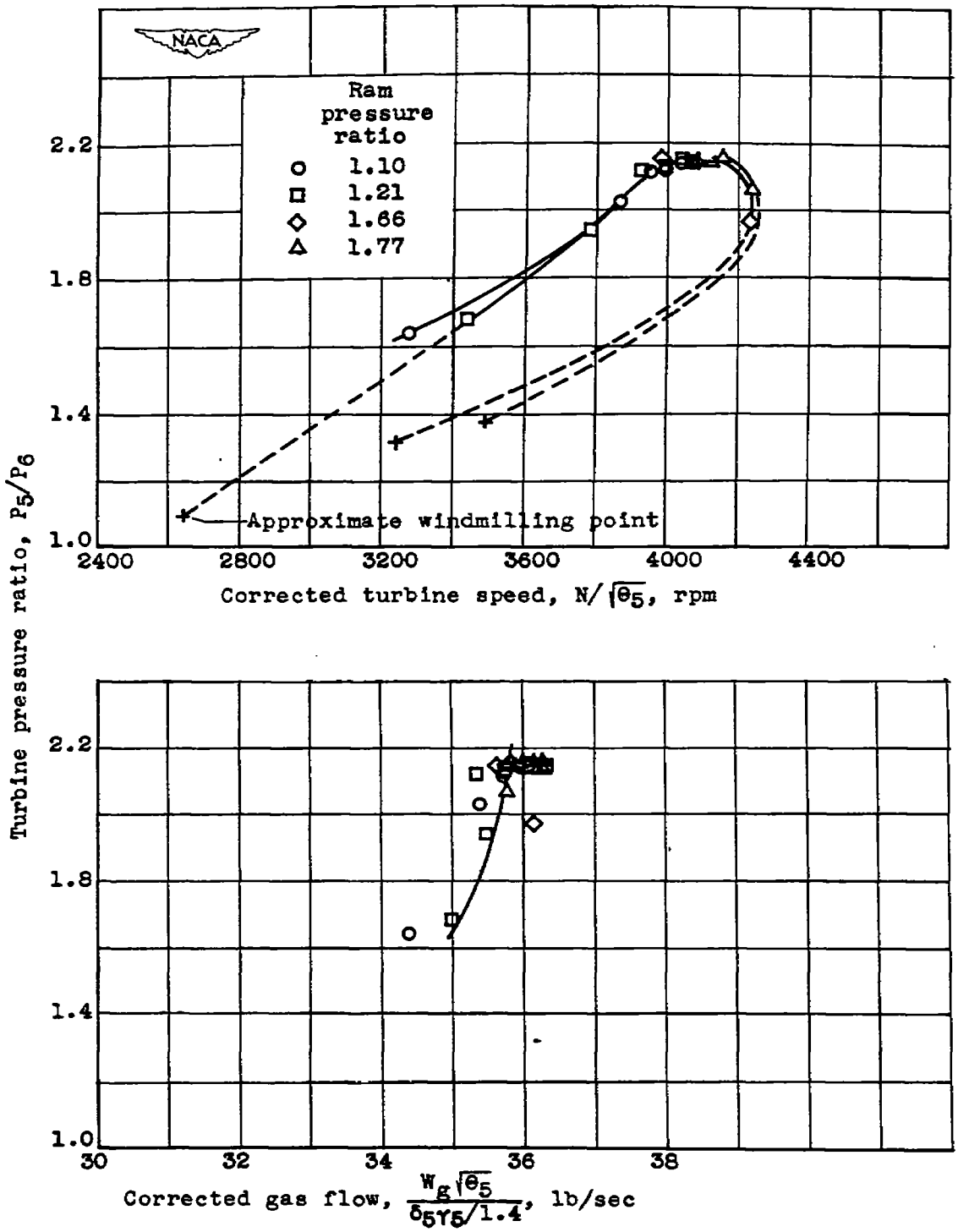

Figure 8.- Effect of ram pressure ratio on turbine operating characteristics with standard turbine nozzle, low-flow compressor, and 16½-inch tail-pipe nozzle at a pressure altitude of 30,000 feet. Turbine speed and gas flow corrected to NACA standard atmospheric conditions at sea level.

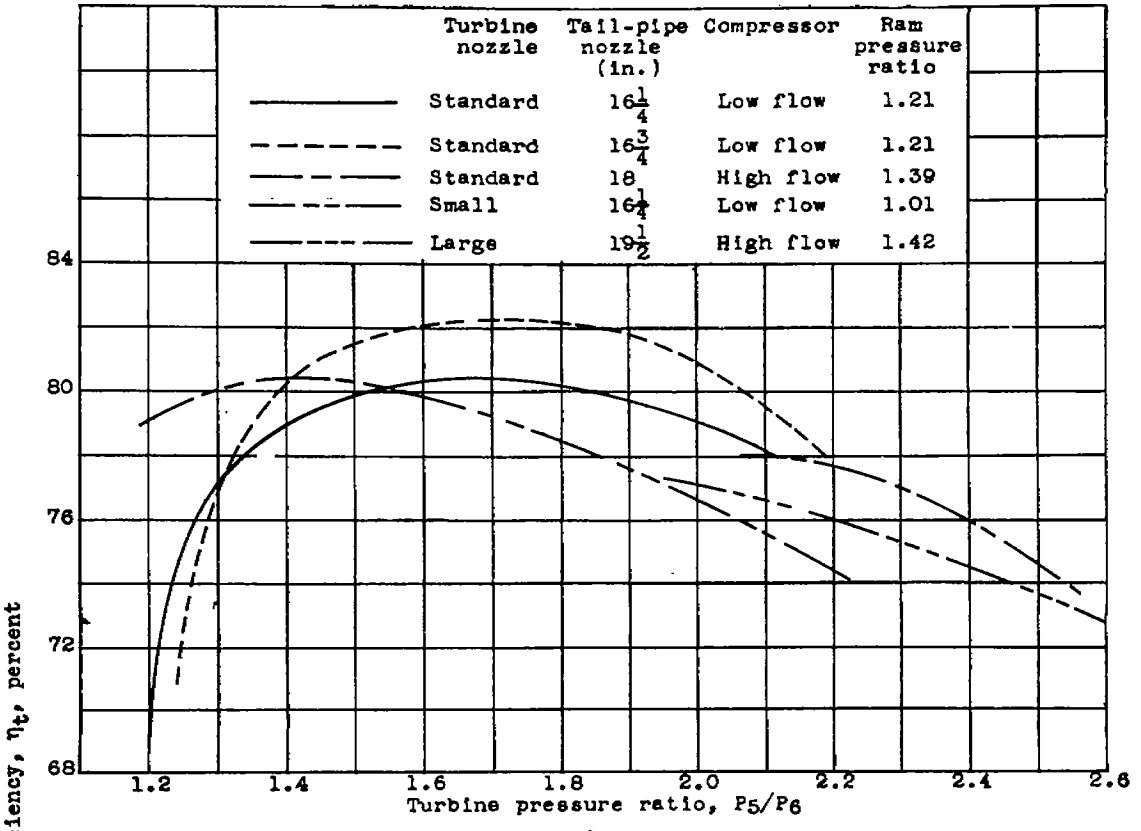

(a) Variation with turbine pressure ratio.

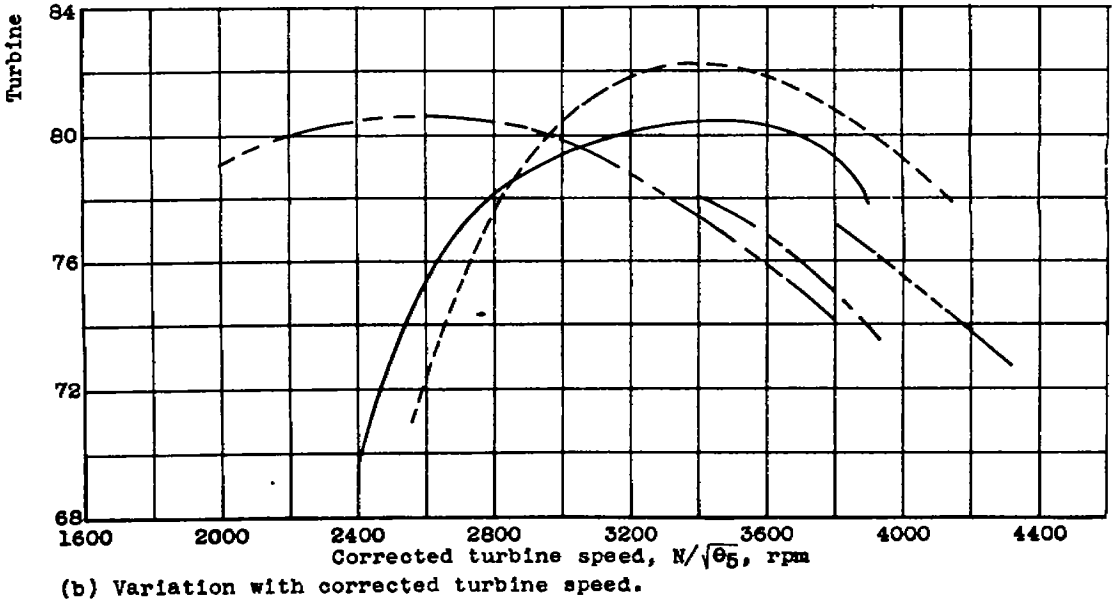

(b) Variation with corrected turbine speed.

Figure 9 .- Variation of turbine efficiency with turbine pressure ratio and corrected turbine speed. Turbine speed corrected to NACA standard atmospheric conditions at sea level.

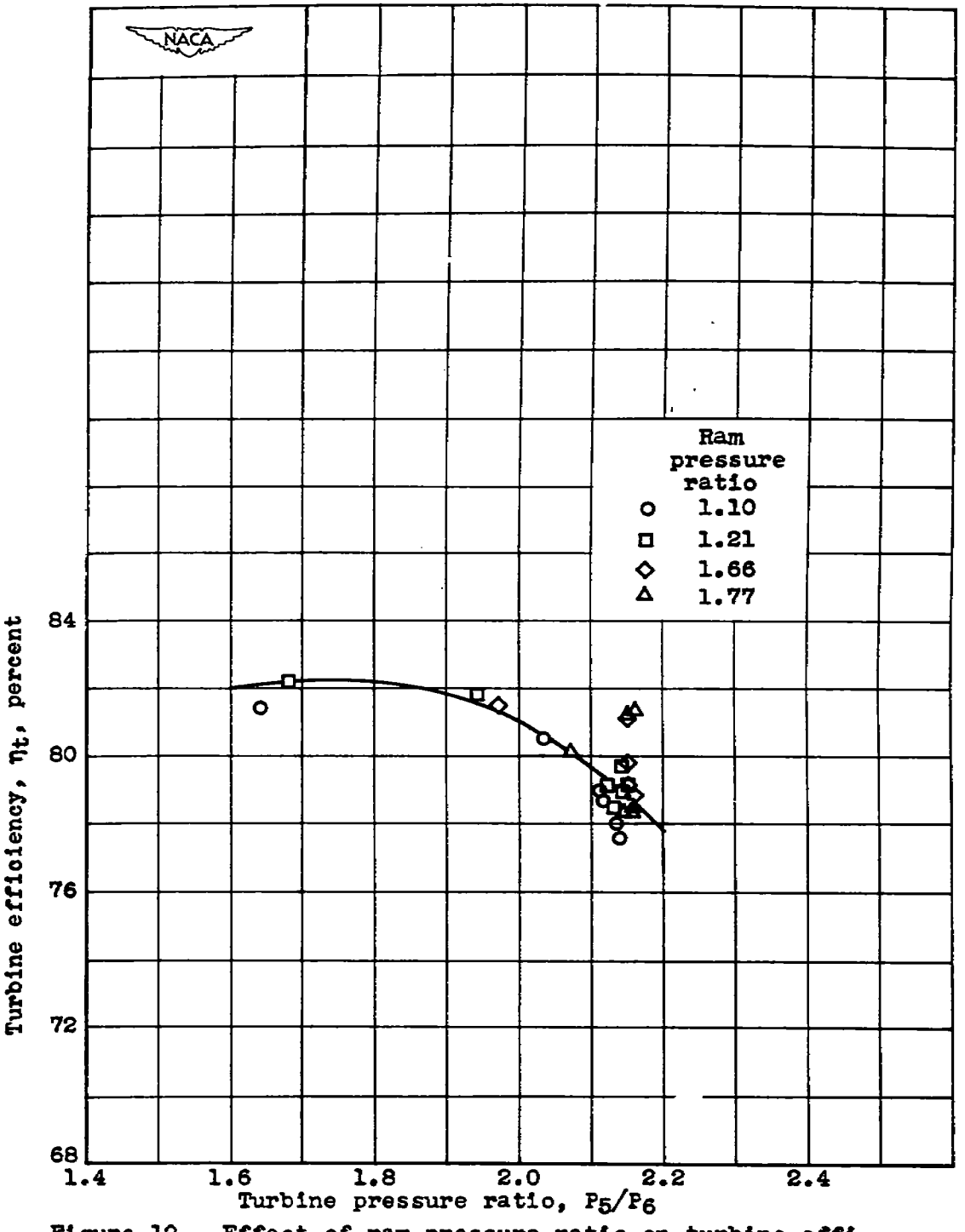

Figure 10.- Effect of ram pressure ratio on turbine efficiency, η_t, with standard turbine nozzle, low-flow compressor, and 16$\frac{3}{4}$-inch tail-pipe nozzle at a pressure altitude of 30,000 feet.